Materials Research Bulletin 87 (2017) 102–108

Contents lists available at ScienceDirect

Materials Research Bulletin

journal homepage: www.elsevier.com/locate/matresbu

Femtosecond third order optical nonlinearity and optical limiting studies of (γ and β)—Barium borate nanostructures

T.C.Sabari Girisun[a,*], R.Madhura Somayaji[b], N.Priyadarshani[a], S.Venugopal Rao[b]

[a] Nanophotonics Laboratory, School of Physics, Bharathidasan University, Tiruchirappalli, India
[b] Advanced Centre of Research in High Energy Materials (ACRHEM), University of Hyderabad, Hyderabad 500046, Telangana, India

ARTICLE INFO

Article history:
Received 22 April 2016
Received in revised form 31 October 2016
Accepted 14 November 2016
Available online 16 November 2016

Keywords:
Nanostructures
Chemical synthesis
X-ray diffraction
Electron microscopy
Optical properties

ABSTRACT

Single phase (γ and β) barium borate with nanorod structures were prepared by hydrothermal method at reaction conditions of 433 and 1073 K, respectively. FESEM images demonstrated the transformation of nanoclusters into elongated nanorods as the reaction time increased. The third order nonlinear optical (NLO) properties of the samples were investigated by the Z-scan technique (800 nm, 150 fs, 100 MHz). Both phases of barium borate depicted nonlinear absorption and was assigned to the two-photon absorption mechanism. γ–BBO demonstrated negative nonlinear refraction (self-defocusing) while β-BBO showed positive nonlinear refraction (self-focusing). Both the phases exhibited optical limiting behavior and the limiting threshold was found to be in the order of μJ/cm^2. Nanorods possessed superior third order NLO coefficients compared to nanoclusters of barium borate. Also γ–BBO possessed superior NLO properties compared to β–BBO and it can be strongly emphasized that γ–BBO nanorods can be used as a potential material for photonic applications.

1. Introduction

Pulsed laser systems are now commonly used in several applications like laser assisted cataract surgery, photo written optical waveguides, micro structuring, ornamental granite cleaning, cancer photo-therapy, etc. [1–5]. In particular, ultrashort pulse lasers have received recent attention in micro-structuring applications as it avoids the breakdown of materials through thermal and mechanical stresses. Moreover ultrashort pulses exhibits high spatial resolution than other conventional lasers and hence ultrashort pulse lasers in femtosecond (fs) scale, even with lower energies can produce the higher order nonlinear optical (NLO) effects [3,6]. This development of high energy density femtosecond (fs) lasers in turn increases the risk of handling it, as even a minimum energy can damage the retina and photosensitive components easily. Thus protection from such highly intense laser is not only of scientific interest but it is also a solution for potential safety issue. The above mentioned problem can be addressed by smart materials called as optical limiters, that exhibit nonlinear extinction i.e. strongly attenuate potentially dangerous laser beams, while readily transmitting low-intensity ambient light [7]. The ideal optical limiters must possess high linear transmission, good resistance to laser induced damage, robustness, fast response, low limiting threshold and neutral calorimetry. Furthermore, novel NLO materials (particularly nanomaterials) with superior coefficients and performance have been investigated by several research groups seeking applications in the fields of optical switching and processing. In the search of photonic materials in general, and efficient optical limiters in particular, one dimensional nanomaterials have been found to be prospective candidates due to their unique optical properties [8,9]. Moreover, the intrinsic anisotropic nature of 1D nanomaterials, resulting from the nanoscale confinement in two dimensions and capability of efficient transport of optical excitations make them attractive compared to bulk materials [10]. Especially nanostructured borate materials have attracted huge attention because of its strategic arrangement of highly NLO active structural units. Barium borate (BBO) is one of the important NLO material which possess the peculiar properties for optical limiting like wide transparency range (190–3500 nm), large birefringence, large nonlinear coefficients ($6 \times d_{eff}$ than KDP at 1064 nm) and high laser damage threshold (5 GW/cm^2 for 10 ns pulses at 1064 nm) [11]. This polymorphic barium borate exists in three form depending upon its reaction temperature, i) barium polyborate i.e., γ- BBO (below

* Corresponding author at: Dr. T.C.Sabari Girisun, Assistant Professor, School of Physics, Bharathidasan University, Tiruchirappalli, 620 024, India.
E-mail addresses: sabarigirisun@bdu.ac.in, sabari.girisun@gmail.com (T.C.S. Girisun), soma_venu@uohyd.ac.in (S.V. Rao).

http://dx.doi.org/10.1016/j.materresbull.2016.11.022
0025-5408/

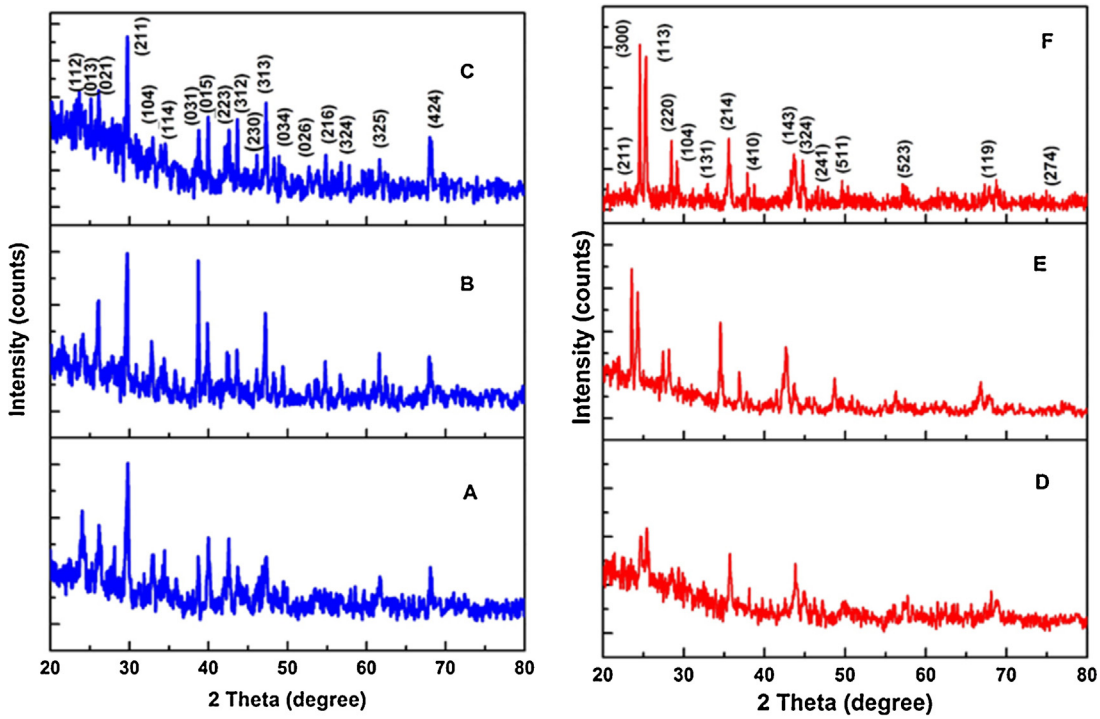

Fig. 1. XRD Pattern of the samples obtained at 433 K for (A) 8, (B) 24, (C) 48 h and at 1073 K for (D) 8, (E) 24, (F) 48 h.

673 K, ii) β- barium borate (673–1223 K), and iii) α- barium borate (above 1223 K) [12]. It is interesting to note that barium borate exists in powder form up to 1223 K and further annealing to higher temperature turns the material to glassy form. Hence most of research is focused on β-BBO nanostructures and reports show that nanorods, nanoplates and network like structures of β-BBO exhibits higher SHG performance than bulk form [13–15].Our recent results [12] demonstrated that γ-BBO nanostructure exhibited higher third order nonlinearities in the continuous wave (CW) and pulsed (nanosecond) regime demonstrating maximum thermal stability against intense laser radiations among the known NLO materials and hence rendering them ideal for optical limiting applications. In continuation with our earlier efforts, this article reports the third order NLO properties and optical limiting behavior of γ- BBO and β-BBO nanorods studied by the standard Z-scan technique using ultrafast laser pulse excitation (800 nm, 150 fs, 80 MHz).

2. Experimental details

Hydrothermal technique was adopted to prepare various nanostructures of γ- BBOand β-BBO by altering the reaction time. In a typical reaction, 4.396 g of $BaCl_2{\cdot}2H_2O$, 1.669 g of H_3BO_3 and 1.439 g of NaOH were dissolved in 108 ml of distilled water and stirred for 2 h to form clear solution. In a stainless steel autoclave, the white slurry was maintained at 433 K for 8 h using a muffle furnace. The obtained flocculent precipitate was filtered using a filter paper and washed repeatedly with distilled water and ethanol to improve its purity. To modify the morphology of the prepared material, similar synthesis procedure was adopted with change in reaction time as 24 and 48 h. Based on the data available from literature [17], to attain the β- phase of barium borate, synthesized powders (obtained at 8, 24 and 48 h) were annealed at 1073 K for 1 h. The samples obtained at 433 K and 1073 K for 8, 24, 48 h were indexed as A, B, C, D, E, F respectively for further analysis. The diffraction pattern of the synthesized powders were obtained by PAN Analytical X-Ray powder diffractometer with a scanning rate of 0.02° s^{-1} in the 2θ range from 20° to 80°. The morphologies of the as-synthesized products were characterized by FEI Quanta FEG 200 High Resolution Scanning Electron Microscope (FESEM). The linear optical absorption spectra were recorded for γ-BBO and β-BBO dispersed in ethylene glycol at room temperature (303 K) with UV–vis spectrophotometer (Perkin Elmer). The third order optical nonlinearity of the dispersed samples (5 mg dispersed in 5 ml of ethylene glycol with a linear transmittance of about 70%) was studied by Z-scan technique using Ti: Sapphire laser (Chameleon) operating at a repetition rate of 80 MHz with pulse duration of ∼150 fs at 800 nm as the excitation source. Typically 2–4 mW input power was used for the experiments. The details of experimental setup and procedure followed in the Z-scan experiment are reported elsewhere [18–21]. Due to the high repetition rate of the laser pulses used (80 MHz) thermo-optic effects like thermal lensing will contribute partially for the observed optical nonlinearity [22].

3. Results and discussion

Fig. 1A–F depict the recorded powder XRD patterns of samples obtained at 433 K and 1073 K for 8, 24, 48 h. All the peaks were indexed and pure single phase BBO was obtained in both the cases. The recorded XRD patterns for γ-BBO (Fig. 1A–C) were matched with JCPDS No. 01-071-2501 and β-BBO (Fig. 1D–F) with JCPDS No. 80-1489 [14,16][14,1012,16]. Elevating the annealing temperature to 1073 K resulted in the formation of pure β-BBO, without any traces of γ-BBO. The pattern clearly indicates that due to the consequent increase in annealing temperature, crystalline nature of the sample got improved. The estimated lattice parameters from the recorded XRD pattern using AUTOX software are given in Table 1 and found to be consistent with the already reported values [14,10,12,16]. It is interesting to note that the crystal structure of γ-BBO is made up of non-planar six-membered B_3O_3 ring built up to form $[B_6O_9(OH)]_n^{6n-}$ anionic infinite chains shared by B atoms with Ba^{2+} cations residing between adjacent chains through electrostatic interaction [23]. While the structure of β-BBO is made

Table 1
Lattice parameters of γ-BBO and β-BBO.

Phase	a (Å)	b (Å)	c (Å)	α (°)	β (°)	γ (°)	Volume (Å^3)	Space Group
γ-BBO	6.98	7.13	11.92	90	90	90	594.32	P2/c
β-BBO	12.53	12.53	12.73	90	90	120	1731.1	R_3C

up of delocalized Π – type bonds which align perpendicular to the [BO_3] plane where the planar BO_3 units condensed to form perfectly oriented [B_3O_6] ring [9–11].

The recorded FESEM images of the samples are shown in Fig. 2. In both the cases, the transformation of aggregated nanoclusters into elongated nanorods with increase in reaction time was observed. As the reaction time increased from 8 to 48 h, prolonged pressure applied upon the particles resulted in the growth of rods along a particular direction, which can be witnessed by the variation in aspect ratio. In the case of γ-BBO, FESEM image of the samples obtained at 433 K for 8 h (Fig. 2A) clearly shows, the energy favored sites offers nucleation and the precipitate exhibit intermolecular force to form larger structure i.e., like bunch of aggregated nanorods. On increasing the time to 24 h (Fig. 2B), transformation from aggregated nanorods to form elongated nanorods with average length and diameter of 1.2 μm and 354 nm takes place to lower the surface energy. Further due to the prolong pressure applied on the nanorods elongation occurs along a particular direction. The image of samples obtained at 48 h (Fig. 2C) shows well defined individual nanorods with average length and diameter of 1.43 μm and 295 nm. A similar transformation with slight variation was also observed in the FESEM images ofβ-BBO. FESEM images for sample obtained at 8 h (Fig. 2D) depicts the formation of agglomerated nanoclusters with size ranging from 65 to 140 nm. This behavior may be due to the aggregation of nuclei together through intermolecular Vander Waal's forces to form nanoclusters. At 24 h (Fig. 2E), clusters continue to grow or elongate in length rather than in width with average length and diameter of 1.48 μm length and 918 nm. At higher reaction time of 48 h (Fig. 2F), individual long range ordered nanorods well grown along the fast growing with average dimension of 1.7 μm length and 209 nm diameter were obtained. The length to diameter aspect ratio was found to be maximum for structures obtained at reaction time of 48 h. Thus FESEM images clearly reveal that reaction time and temperature plays a major role in the formation of nanostructures [24,25].

Z-scan technique is a powerful method in which near to the focal point, the variation of transmission against the incident intensity gives the information about the third order NLO properties of the material. In both open (without aperture) and closed (with aperture) mode, the total nonlinear transmittance through the sample was measured while the sample is translated along the direction of propagating laser beam. In general, if the incident photon energy is greater than the band gap energy of the material, the sample exhibits saturable/reverse saturable absorption resulting from ground state to excited transition state. Moreover if the incident photon energy is less than the band gap of the material, it will not have the sufficient energy to excite the electrons directly to the excited state, therefore two photons got simultaneously absorbed i.e., two photon absorption occurs [26]. The standard nonlinear transmission equation was used to calculate the nonlinear coefficients by numerically fitting the measured Z-scan curve.

The recorded open aperture (OA) patterns for the samples investigated are shown in Fig. 3, in which the valley indicates a decrease in transmission at the focal point confirming the nonlinear behavior of the sample. The depth of the valley signifies the extent of NLO performance and the shoulder indicates the behavior at low input fluence (far away from the focus represents the linear transmittance, which is constant). In both the cases, the valley was found to be deeper for the samples obtained at 48 h and thereby confirming the superiority of nanorods in attaining higher NLO behavior. In the pattern, open circles represent the measured data points and solid lines correspond to the theoretical fit drawn based on Sheik-Bahae formalism [27]. The numerical simulation

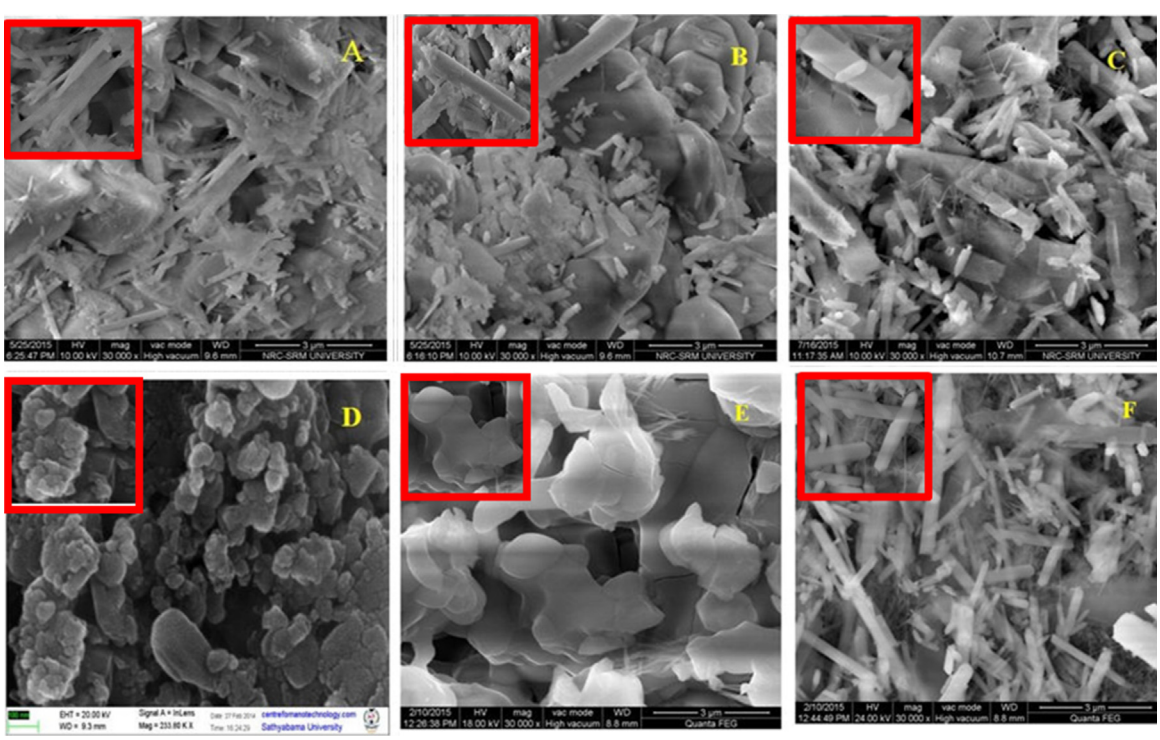

Fig. 2. Morphology of γ-BBO obtained at (A) 8, (B) 24, (C) 48 h and β-BBO obtained at (D) 8, (E) 24, (F) 48 h.

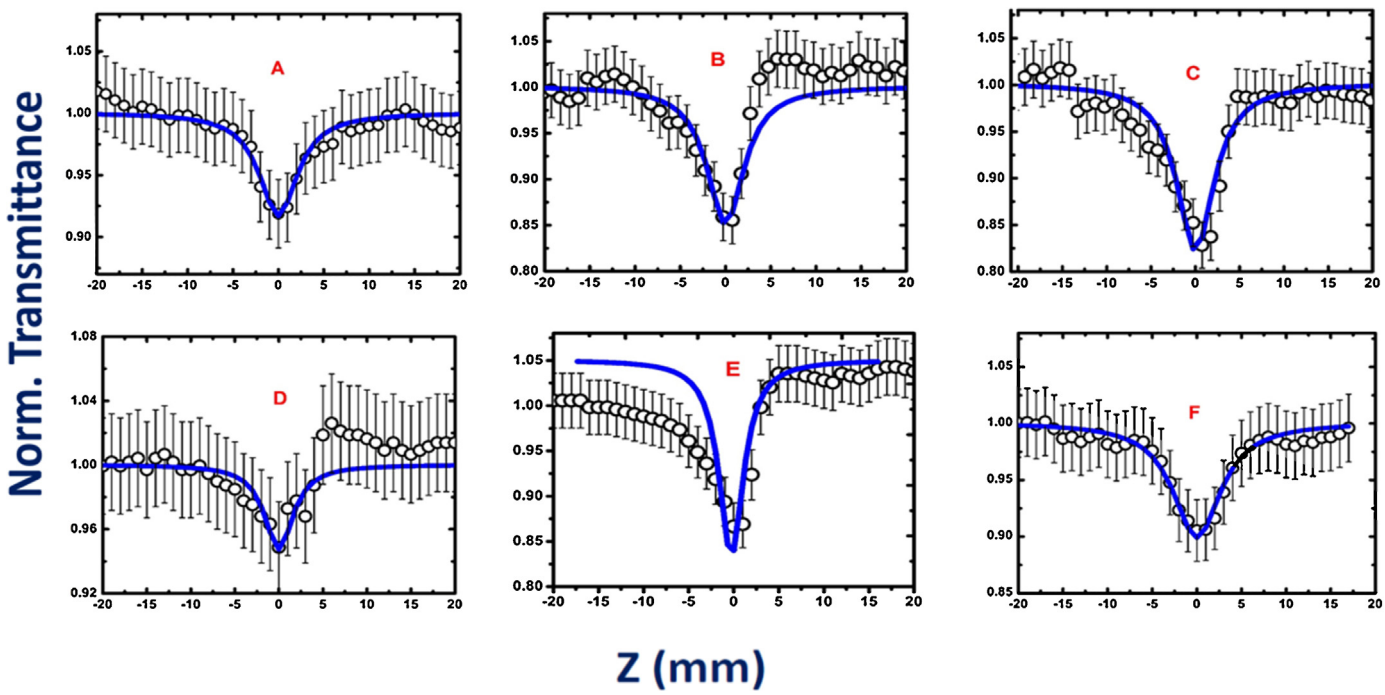

Fig. 3. Open aperture Z-scan data of γ-BBO obtained at (A) 8, (B) 24, (C) 48 h and β-BBO obtained at (D) 8, (E) 24, (F) 48 h.

for the obtained experimental data was found to be best fit for two photon absorption (2PA) process [28] using the equation

$$T(z,S=1)=\frac{1}{\sqrt{\pi}q_0(z,0)}\int_{-\infty}^{\infty} ln\left[1+q_0(z,0)e^{-\tau^2}\right]d\tau \quad (1)$$

where T (z) is the normalized transmittance as a function of z, $q_0=\beta L_{eff}I_0$ where β is the 2PA coefficient, I_0 is the peak intensity at focus. The recorded UV–vis absorption spectra of the barium borate nanorods dispersed in the ethylene glycol (provided in the Supplementary data), clearly shows a strong absorption band in the vicinity of 210–230 nm. Literature data suggests that BBO crystal depicts transparency even below 190 nm and is used for the tunable deep UV laser generation [29–31]. Red shift in the absorption maxima for BBO nanorod (dispersed in liquid media) compared to crystal can be attributed to specific solute-solvent interaction in the form of hydrogen bonding [32]. The variation in the absorption maxima between present and reported BBO nanorod [33] could be due to the change in polarity of the solvent. As the relative polarity of ethylene glycol (0.79) is higher than ethanol (0.65), the dispersed BBO nanorods have suffered a bathochromic shift [32]. Both γ-BBO and β-BBO depicted a strong emission at 347 nm in its PL spectrum which corresponds to the presence of self-trapped exciton state [12,16]. With ultrashort pulse excitation (800 nm, 1.55 eV, ~150 fs) the electrons in the lowest state could possibly be excited to the self-trapped exciton state by simultaneously absorbing two photons (1.55 eV) accompanied by sequential absorption of energy through non-radiative process (preferably thermal, due to high repetition rate) [34,35]. Hence, the observed nonlinearity can mainly be attributed to the 2PA process. It is well established that the population in the excited state (if it is a real/Eigen state) stays longer than the pulse duration. There is no scope for excited state absorption with such short laser pulses. The estimated effective nonlinear absorption coefficient (β_{eff}) of the samples is tabulated in Table 2. It is interesting to note that nonlinear absorption coefficient is found to be higher for γ-BBO than β-BBO.

The high nonlinearity for γ-BBO is due to the peculiar structural arrangement it possess among the various borate materials. γ-BBO is the only chain borate material solely made up of BO_4 tetrahedral anionic groups [23], while β-BBO is made up of both BO_3 and BO_4 unit [36]. Gradual increase in β_{eff} with reaction time clearly shows the role of aspect ratio of the rods and elongated individual nanorods obtained at 48 h has maximum value than other structures. In particular, γ-BBO nanorods with higher aspect ratio possess high nonlinear absorption coefficient compared to other NLO materials like, CdSe quantum dots (4.1×10^{-15} m/W) [36], graphene oxide (4×10^{-10} m/W) [37], RGO suspension (25×10^{-12} m/W) [38], CdO nanoflakes (6.9×10^{-15} m/W) [39] and Fe_2O_3 hexagonal nanostructures (8.2×10^{-15} m/W) [40] investigated under similar experimental condition (80–150 fs). Two-photon absorption co-efficient of BBO

Table 2
Third order NLO parameters extracted from Z-scan studies.

Sample	n_2 $\times10^{-12}$ $cm^2 W^{-1}$	β_{eff} $\times10^{-10}$ cm W^{-1}	Re $\chi^{(3)}$ $\times10^{-10}$ e.s.u	Im $\chi^{(3)}$ $\times10^{-12}$ e.s.u	Total $\chi^{(3)}$ $\times10^{-10}$ e.s.u	Onset Limiting threshold μJ/cm^2
A	3.1	750	1.5	2.3	1.5	0.39
B	4.9	1670	2.4	5.2	2.4	0.36
C	10.3	1993	5.0	6.2	5.0	0.29
D	0.3	210	0.2	0.9	0.2	0.50
E	1.0	650	0.7	2.9	0.7	0.39
F	3.1	950	2.2	4.3	2.2	0.31

crystal (68×10^{-11} cm/W), liquid BBO (95×10^{-11} cm/W) and glassy BBO (9.4×10^{-11} cm/W) [41] obtained using fs excitation ($\lambda = 264$ nm, 200 μJ) was found to be smaller than the reported value here. However, since the data obtained from Z-scan experiments are very sensitive to the experimental parameters such wavelength, phase width, frequency and power, direct correlation is not possible. It is worthy to be noted that the larger value of the present samples are also due to the inclusion of thermal nonlinearity arising from higher repetition rate (80 MHz) of laser employed.

The recorded closed aperture (CA) patterns are shown in Fig. 4. It is interesting to note that the pattern observed is not identical for both the phases. γ-BBO exhibited valley followed by peak pattern, i.e., self-focusing showing positive nonlinearity of the sample. The data of β-BBO clearly depicted a peak followed by valley pattern, i.e., self-defocusing suggesting a negative nonlinearity in the sample. In the patterns, the open circles represent the measured data points and solid lines correspond to the theoretical fit drawn based on Sheik-Bahae formalism. To evaluate the nonlinear refractive index of the materials, first the normalized closed aperture transmittance (T_{CA}) was estimated, using a standard relation given as

$$T_{CA} = 1 \pm \frac{4\Delta_{\Phi}(\frac{z}{z_0})}{\left[1 + (z/z_0)^2\right]\left[9 + (z/z_0)^2\right]} \quad (2)$$

where ΔØ is the phase change of the laser beam, z is the longitudinal distance moved by the sample from the focus ($z = 0$) and z_0 is the Rayleigh range. The nonlinear refractive index n_2 was calculated using the standard relation [28] and presented in Table 2. It is interesting to see that the sign of nonlinearity changes from positive to negative for high temperature annealed samples. Also the third order nonlinear optical susceptibility, $\chi^{(3)}$ of the materials were calculated using the standard relations [42]. The obtained value shows that nanorods possess higher third order NLO susceptibility than nanoclusters. This is because, anisotropic nature of one dimensional nanorods results in the nanoscale confinement in two dimensions leading to the efficient transport of optical excitations. Also in one dimensional structure the incident field is fully coupled to local mode and hence the optical nonlinearity of the nanorods was effectively enhanced. Moreover the γ–BBO exhibits high third order nonlinearity than β–BBO. The estimated third order nonlinear optical coefficients suggest that the presence of BO_4 basic structural unit in γ–BBO promotes the nonlinear behavior. As like nonlinear absorption coefficient, the order of magnitude of third-order nonlinear optical susceptibility of γ–BBO was higher than β–BBO nanorods.

Limiting threshold is the point at which the input fluence falls to half of the linear transmittance value and the output intensity is constant above the threshold. Moreover it depends upon materials linear transmittance, excitation wavelength and laser pulse width. From open aperture z-scan, the input laser energy density was evaluated using the relation

$$F(z) = \frac{\sqrt{\ln 2}.E_{in}}{\pi^{\frac{3}{2}}.\omega(z)^2} \quad (3)$$

where E_{in} is the input laser energy and ω (z) is the beam radius. Fig. 5 shows the extracted optical limiting pattern of γ- BBO and β-BBO. The solid lines indicates the theoretical fit and the curve reveals under strong fluence the curve departs from Beer's law, i.e., nonlinearity leading to optical limiting behavior. The mechanism for optical limiting is due to the 2PA and moreover the curve depth indicates the higher limiting behavior. For γ- and β-BBO phase, nanorods obtained at 48 h possess low limiting threshold (0.29 and 0.31 μJ/cm^2 respectively) than other structures and γ-BBO has low threshold than β-BBO. Also the limiting threshold of both phases of BBO was found to be lower than other limiting materials like Duran glass (35 μJ) and ZnO thin films (128 μJ/cm^2) irradiated with similar laser [43,44]. Thus it is clear that γ-BBO nanorods (48 h, C) which has high nonlinear absorption coefficient, nonlinear optical susceptibility and low limiting threshold value can be a preferred candidate for high power optical limiting applications with ultrashort laser pulse (800 nm, 150 fs) excitation. The error bars in Figs. 3–5 are due to the errors in (a) the measurement of the spot size, which is critical for calculating the peak intensities (b) the

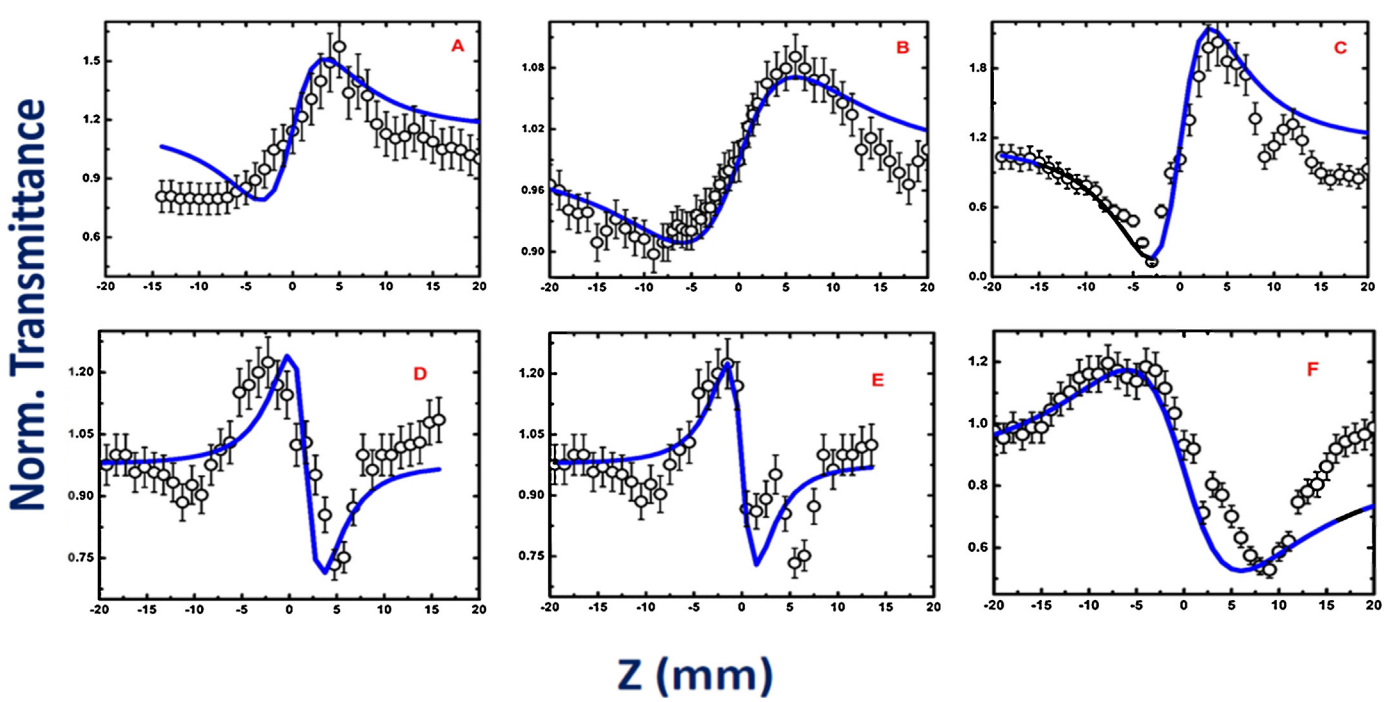

Fig. 4. Closed aperture Z-scan data of γ-BBO obtained at (A) 8, (B) 24, (C) 48 h and β-BBO obtained at (D) 8, (E) 24, (F) 48 h.

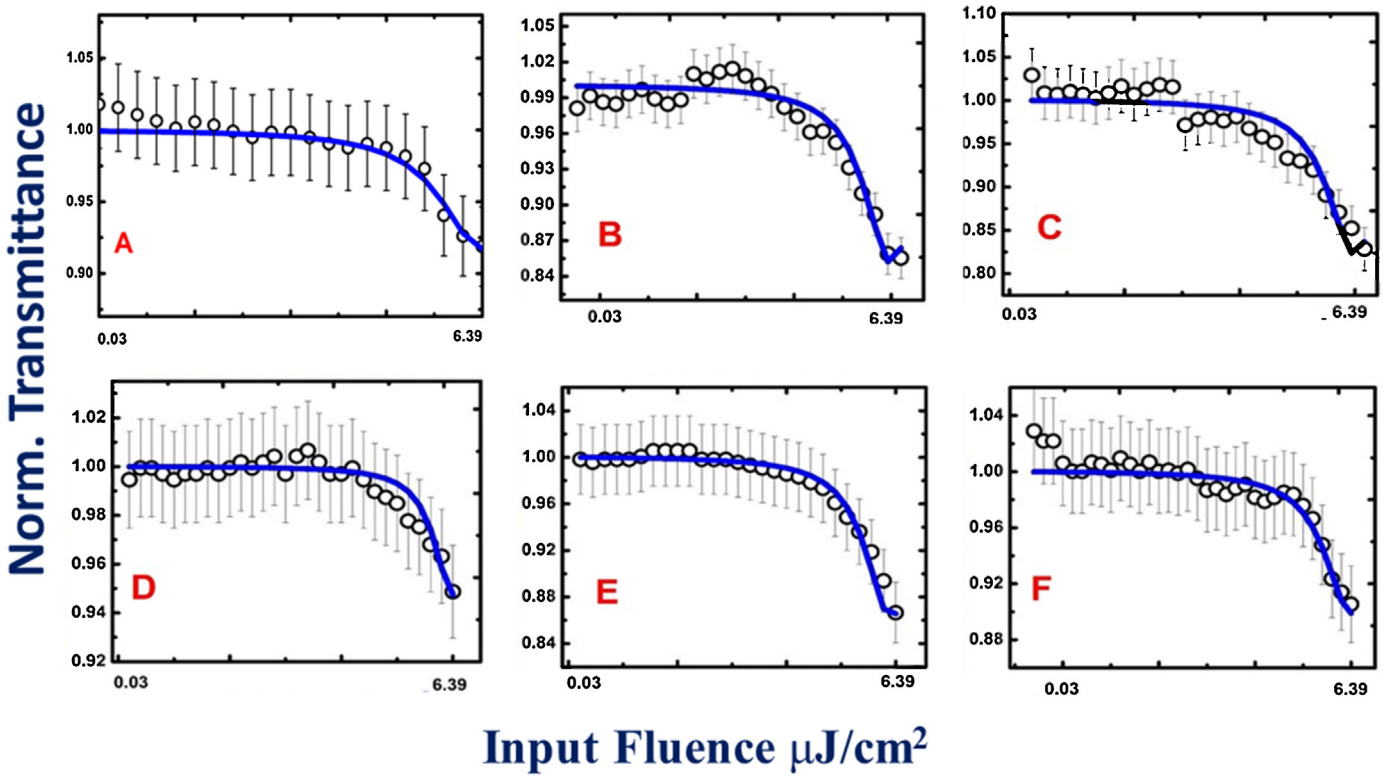

Fig. 5. Optical limiting data of γ-BBO obtained at (A) 8, (B) 24, (C) 48 h and β-BBO obtained at (D) 8, (E) 24, (F) 48 h.

fitting procedures (c) the input laser power/intensity fluctuations and (d) input power measurements.

4. Conclusions

In summary, γ-BBO and β-BBO nanorods were successfully prepared by varying the reaction time (8, 24 and 48 h) in hydrothermal technique. Preliminary confirmation and single phase formation were confirmed by XRD analysis. The FESEM data demonstrated the formation of smooth nanorods with higher aspect ratio of 8.1 at the reaction time of 48 h. The influence of reaction time in altering the morphology was thoroughly discussed. Using Ti: Sapphire laser (800 nm, 150 fs) as excitation source, the third order nonlinear optical properties of (γ- and β-) BBO were studied by Z-scan technique. The observed nonlinearity in the OA patterns show that nonlinear absorption of the materials is due to effective two photon absorption process. Among the materials prepared, γ-BBO nanorods (C) possess nonlinear absorption coefficient of 19.9×10^{-10} m/W which is very higher than the values obtained for some of the well- known nanostructure NLO materials. The large enhancement in effective two photon absorption coefficient is due to peculiar crystal structure of the material i.e., the chain borate is solely made up of BO_4 tetrahedral anionic groups. CA pattern shows the sign reversal in the nonlinear refraction and γ-BBO possessed positive nonlinearity (self-focusing) while β-BBO depicted negative nonlinearity (self-defocusing). The magnitude of nonlinear refractive index and third order NLO susceptibility were calculated and is found to be increasing with increase in reaction time. The estimated third order NLO susceptibility was found to be higher for γ-BBO than β-BBO. In both the phases, as reaction time increase the third order NLO coefficients also increases, which might be due to the increase in aspect ratio. The two photon absorption contributes the optical limiting behavior of alkaline earth borates under femtosecond laser pulses and the limiting threshold is in the range of 0.29–0.50 μJ/cm^2. The result suggests that barium borate nanorods can play a major role in optical limiting applications in femtosecond regime. Further it can be concluded that γ-BBO nanorods (433 K, 48 h) with superior third order NLO coefficients and low limiting threshold value can be a potential candidate for high power optical limiting applications under ultrashort laser (800 nm, 150 fs) pulses.

Acknowledgment

One of the authors S.V. Rao thanks DRDO, India for continued financial support.

Appendix A. Supplementary data

Supplementary data associated with this article can be found, in the online version, at http://dx.doi.org/10.1016/j.materresbull.2016.11.022.

References

[1] Jorge L. Alio, Saudi J. Ophthalmol. 25 (2011) 219–223.
[2] E. Zgraggen, I.M. Soganci, F. Horst, A. La Porta, R. Dangel, B.J. Offrein, S.A. Snow, J.K. Young, B.W. Swatowski, C.M. Amb, O. Scholder, R. Broennimann, U. Sennhauser, G.-L. Bona, J. Lightwave Technol. 32 (2014) 3036–3042.
[3] A.Y. Vorobyev, C. Guo, Laser Photonics Rev. 7 (2013) 385–407.
[4] T. Rivasa, A.J. Lopez, A. Ramil, S. Pozo, M.P. Fiorucci, M.E. López de Silanes, A. García, J.R. Vazquez de Aldana, C. Romero, P. Moreno, Appl. Surf. Sci. 278 (2013) 226–233.
[5] X. Wu, J.-Y. Chen, A. Brech, C. Fang, J. Wang, P.J. Helm, Q. Peng, Biomaterials 34 (2013) 6157–6162.
[6] R.L. Sutherland, Handbook of Nonlinear Optics, Marcel Dekker, 2010.
[7] Liyan Chen, Feifei Chen, Shixun Dai, Guangming Tao, Lihe Yan, Xiang Shen, Hongli Ma, Xianghua Zhang, Yinsheng Xu, Mater. Res. Bull. 70 (2015) 204–208.
[8] P. Jafarkhani, A. Chehrghani, M.J. Torkamany, Mater. Res. Bull. 47 (2012) 608–613.

[9] P. Thomas, P. Sreekanth, R. Philip, K.E. Abraham, RSC Adv. 5 (2015) 35017–35025.
[10] A.L. Tiano, C. Koenigsmann, A.C. Santulli, S.S. Wong, Chem. Commun. 46 (2010) 8093–8130.
[11] P. Becker, Adv. Mater. 10 (1998) 979–992.
[12] C. Babeela, T.C. Sabari Girisun, Opt. Mater. 49 (2015) 190–195.
[13] J. Zhang, G. He, R. Li, X. Chen, J. Alloys Comp. 489 (2010) 504–508.
[14] C. Lu, R.H. Lipson, CrystEngComm 12 (2010) 4352–4355.
[15] Q. Zhao, X. Zhu, X. Bai, H. Fan, Y. Xie, Eur. J. Inorg. Chem. 2007 (2007) 1829–1834.
[16] C. Babeela, T.C.S. Girisun, G. Vinitha, J. Phys. D: Appl. Phys. 48 (2015) 065102–065109.
[17] A. Garai, S. Kumar, W. Sinha, C.S. Purohit, R. Das, S. Kar, RSC Adv. 5 (2015) 28643–28651.
[18] D. Swain, A. Rana, P.K. Panda, S. Venugopal Rao, Chem. Phys. Lett. 310 (2014) 610–611.
[19] D. Swain, T. Sarma, P.K. Panda, S. Venugopal Rao, Chem. Phys. Lett. 580 (2013) 73.
[20] D. Swain, R. Singh, V.K. Singh, N.V. Krishna, L. Giribabu, S. Venugopal Rao, J. Mater. Chem. C 2 (2014) 1711–1722.
[21] N.V. Krishna, V.K. Singh, D. Swain, S. Venugopal Rao, L. Giribabu, RCS Adv. 5 (2015) 20810.
[22] G. Zhou, W.-Y. Wong, S.-Y. Poon, C. Ye, Z. Lin, Adv. Funct. Mater. 19 (2009) 531–544.
[23] Z.-T. Yu, Z. Shi, W. Chen, Y.-S. Jiang, H.-M. Yuan, J.-S. Chen, J. Chem. Soc. Dalton Trans. (2002) 2031–2035.
[24] L. Bao, Z.-H. Xu, R. Li, X. Li, Nano. Lett. 10 (2010) 255–262.
[25] Y. Xia, P. Yang, Y. Sun, Y. Wu, B. Mayers, B. Gates, Y. Yin, F. Kim, H. Yan, Adv. Mater. 15 (2003) 353–389.
[26] K. Wang, Y. Feng, C. Chang, J. Zhan, C. Wang, Q. Zhao, J.N. Coleman, L. Zhang, W. J. Blau, J. Wang, Nanoscale 6 (2014) 10530–10535.
[27] M. Sheik-Bahae, A.A. Said, T.-H. Wei, D.J. Hagan, E.W. Van Stryland, J. Quantum Electron. 26 (1990) 760–770.
[28] S. Hamad, Surya P. Tewari, L. Giribabu, S. Venugopal Rao, J. Porphyrins Phthalocyanines 16 (2012) 140.
[29] Rashid A. Ganeev, Nonlinear Optical Properties of Materials, Springer, 2013.
[30] M. Bache, H. Guo, B. Zhou, X. Zeng, Opt. Mater. Exp. 3 (2013) 357–382.
[31] G.C. Bhar, U. Chatterjee, A.M. Rudra, P. Kumbhakar, R.K. Route, R.S. Feigelson, Opt. Lett. 22 (1997) 1606–1608.
[32] M. Homocianu, A. Airinei, D. Ortansa Dorohoi, J. Adv. Res. Phys. 2 (2011) 011105.
[33] J. Zhang, G. He, R. Li, X. Chen, J. Alloys Comp. 489 (2010) 504–508.
[34] E.D. D'silva, G. Krishna Podagatlapalli, S. Venugopal Rao, S.M. Dharmaprakash, Mater. Res. Bull. 47 (2012) 3552–3557.
[35] Xinyu Yang, Weidong Xiang, Haijun Zhao, Xiyan Zhang, Xiaojuan Liang, Shixun Dai, Feifei Chen, Mater. Res. Bull. 46 (2011) 355–360.
[36] Jian Liu, Mater. Res. Bull. 81 (2016) 114–118.
[37] V. Sreeramulu, K.K. Haldar, A. Patra, D. Narayana Rao, J. Phys. Chem. C 118 (2014) 30333–30341.
[38] S. Kumar, N. Kamaraju, K.S. Vasu, A. Nag, A.K. Sood, C.N.R. Rao, Chem. Phys. Lett. 499 (2010) 152–157.
[39] P. Thomas, P. Sreekanth, R. Philip, K.E. Abraham, RSC Adv. 5 (2015) 35017.
[40] P. Thomas, P. Sreekanth, K.E. Abraham, J. Appl. Phys. 117 (2015) 053103–053108.
[41] A. Dragonmir, John G. McInerney, David N. Nikogosyan, Appl. Opt. 41 (2002) 4365–4376.
[42] S.J. Mathews, S. Chaitanya Kumar, L. Giribabu, S. Venugopal Rao, Opt. Commun. 280 (2007) 206–212.
[43] K. Jamshidi-Ghaleh, N. Mansour, J. Phys. D: Appl. Phys. 40 (2007) 366–369.
[44] U. Pasha Shaik, P. Ajay Kumar, M. Ghanashyam Krishna, S. Venugopal Rao, Mater. Res. Express 1 (2014) 046201.